An integrated method for the transient solution of reduced order models of geometrically nonlinear structures

Fritz Lülf, Duc-Minh Tran, Hermann G. Matthies, Roger Ohayon

An integrated method for the transient solution of reduced order models of geometrically nonlinear structures

Fritz Adrian Lülf, **Duc-Minh Tran**,
Hermann G. Matthies, **Roger Ohayon**

Abstract For repeated transient solutions of geometrically nonlinear structures, the numerical effort often poses a major obstacle. Thus it may become necessary to introduce a reduced order model which accelerates the calculations considerably while taking into account the nonlinear effects of the full order model in order to maintain accuracy. This work yields an integrated method that allows for rapid, accurate and parameterisable transient solutions. It is applicable if the structure is discretised in time and in space and its dynamic equilibrium described by a matrix equation. The projection on a reduced basis is introduced to obtain the reduced order model. Three approaches, each responding to one of the requirements of rapidity, accuracy and parameterisation, are united to form the integrated method. The polynomial formulation of the nonlinear terms renders the solution of the reduced order model autonomous from the finite element formulation and ensures a rapid solution. The update and augmentation of the reduced basis ensures the accuracy, because the simple introduction of a constant basis seems to be insufficient to account for the nonlinear behaviour. The interpolation of the reduced basis allows adapting the reduced order model to different external parameters. A Newmark-type algorithm provides the backbone of the integrated method. The application of the integrated method on test-cases with geometrically nonlinear finite elements confirms that this method enables a rapid, accurate and parameterisable transient solution.

Keywords Structural dynamics · Geometric nonlinearities · Model reduction · Reduced bases · Normal modes · Tangent modes · Basis update · Parameters

F. A. Lülf (✉) · D.-M. Tran
ONERA, The French Aerospace Lab, 92322 Châtillon, France

Present Address:
F. A. Lülf
Institute of Continuum Mechanics, Leibniz Universität Hannover, Appelstr. 11, 30167 Hannover, Germany
e-mail: luelf@ikm.uni-hannover.de

H. G. Matthies · R. Ohayon
Institut für Wissenschaftliches Rechnen, Technische Universität Braunschweig, 38092 Braunschweig, Germany

R. Ohayon
Structural Mechanics and Coupled Systems Laboratory, Conservatoire National des Arts et Métiers, 2 rue Conté, 75003 Paris, France

1 Introduction

In the domain of structural dynamics reduced order models (ROM) can be desirable for various reasons. They can, for example, be used to reduce the computational burden in a design process, they can be designed as fast executing replacements of the full order model (FOM) in embedded control applications, or they can be used to extract pertinent information which is hidden in the FOM. Irrespective of the aim pursued with it, the ROM is never an end in itself. In the context of this work development is geared towards gaining computational speed.

There are at least two different approaches to model reduction. One is the so-called goal-oriented reduction approach. It is applied by e.g. [7]. In their work, the entire FOM is directly reduced to the cost-function that is required for an optimisation. This cost-function does not contain any information about the physical properties of the FOM. This is opposite to the physical reduction approach, which is applied in this work. Here, the central property of a ROM is the fact that the ROM does not change the physics of the underlying problem.

In this work, the ROM is to be used for establishing the transient response of a geometrically nonlinear, non-conservative structure to an external excitation evolving in time. Against the given requirements and with a strong emphasis on the anticipated needs for adapting the most modular reduction approach, the approach of the projection on a reduced basis is chosen. A flat subspace is defined, represented by the reduced basis $\mathbf{\Phi}$, which is used as a basis onto which the discrete equation, describing the nonlinear dynamic system, is projected. Besselink et al. [6] point out that the reduction by projection approach is by far the approach requiring the most intervention, knowledge and experience from its user. This fact is exploited to integrate the selected methods seamlessly, while retaining the character of the integrated method, as it presented here, as just one realisation of a more general framework.

The system is discretised in time and in space. The time-marching solution algorithm, required for establishing the transient solution, is the backbone of integrated method. Different members of the family of linear multi-step methods, e.g. Newmark-type time-marching algorithms [29], can be used. Because of the fact that the FOM and the ROM have the exact same structure both descriptions of the system's dynamics can be solved by the same algorithm.

The trade-off between gain in computational effort and error committed defines the success of the application of the ROM. Both criteria are explored further over the course of this work. The order r of the ROM defines its size and has to be aptly chosen so that the ROM can retain the crucial properties of the FOM. At the same time, however, the computational cost of the necessary transformations between the ROM and the FOM, deflations and inflations, must not exceed the gains through the accelerated solution of the ROM.

The aim of this work is to obtain a rapid, accurate and parameterisable transient solution of a geometrically nonlinear, non-conservative structure. Each of these three aspects is addressed with a specific method. These methods form the elements that constitute the integrated method. The rapid execution of the solution is enabled by ensuring the autonomy of the ROM. The accuracy of the reduced solution is assured with the update and augmentation of the reduced basis. The aspect of the adaptation of the ROM to external parameters is provided with the interpolation of the reduced basis. These three elements are detailed independently from each other in Sect. 3 in order to prepare the creation of the integrated method in Sect. 4. A first, brief presentation is given now.

The autonomous formulation of the nonlinear terms replaces the finite element expressions, which are required during the solution with a sum of tensor-vector-products. A point of central importance of this approach is the identification of the tensors. Mignolet and Soize [27] distinguish between direct and indirect identification approaches. Direct approaches draw on the finite element formulations and obtain the tensors by integration. The drawback of direct approaches is that they require access to the formulation of the finite elements. Indirect approaches identify the tensors by means of combining different static evaluations of nonlinear forces vector with imposed displacements for moment matching. One approach is proposed by [28]. It can be used with any, even a proprietary, finite element code. However, it requires a considerable number of static evaluations of the finite element formulation of the nonlinear internal forces. Should full order tensors be identified, they can be reduced with an approach from [32]. Preceding works with the application of the polynomial formulation include the application of the method by [20] to clamped beams and by [35] for the prediction of sonic fatigue responses.

The update and augmentation of the reduced basis is a procedure which makes the reduced basis follow the nonlinear evolution of the transient solution. The update of the reduced basis is not to be confused with the update of the entire model, which is a common, problematic challenge in the domain of the resolution of inverse problems (e.g. [18] and [11]). The numerical results obtained by [24] strongly suggest that the simple introduction of a constant reduced basis is not sufficient and that an evolution of the reduced basis during the transient solution is necessary. The augmentation of the updated basis with the jumps in the physical quantities is a novel aspect of the common sense approach of updating the reduced basis and an original contribution of this work.

ROM are prone to produce rapidly deteriorating results, if they are applied to operating points that have external parameters further away from the initial parameterisation. This is confirmed by several studies, e.g. [16,17], and by the results of study of the robustness in [24]. As a remedy [2,3] propose an approach for the interpolation of reduced bases, which relies on an interpolation in a tangent space. It allows overcoming the deteriorating results and makes the ROM parameterisable.

There are many more highly specific approaches for each one of the three aspects of a rapid, accurate and parameterisable transient solution. The multitude of methods that have been and are developed around the reduction by projection on a reduced basis offers all elements that are required to respond to the three aims with a dedicated method. Also available are a multitude of different common methods for creating reduced bases and solution algorithms, which take the nonlinear behaviour of the system into account.

However, there seems to be no integrated method that combines such approaches in order to achieve all three aspects at once. In fact, the domain of structural dynamics is lacking a single integrated method that merges approaches for all three aims and provides a consistent framework for combining these approaches [26]. This lack seems to persist already for a certain time [31]. Also, there is no framework

available that allows combining different approaches, each one achieving one aspect, in an interchangeable manner in order to construct an integrated method for a given problem. The primary motivation of this work is providing such a framework and describing an integrated method.

A first tentative approach at combining different methods is made by [12]. They use the harmonic balance method in conjunction with the proper generalised decomposition in order to obtain reduced periodic solutions of geometrically nonlinear structures. Their strive for steady state periodic solution distinguishes their approach from the presented work. Compared to already published works, the originality of the present study resides in the fact that it investigates and names the elements that are necessary to obtain the transient solution of the ROM of a geometrically nonlinear system with an integrated method.

One method that can possibly combine the three aspects is the proper generalised decomposition (PGD). While the approach with reduced bases is a projection of the equation of the dynamic equilibrium of the structure on a flat manifold, the PGD approach is a projection on a curved manifold. This method treats the dimensions of the problem independently from each other in a low-rank tensor approximation and can hence be seen as a separation of variables [13], similar to a dimension reduction of shells and plates [1]. Introducing additional dimensions allows even to treat effects like e.g. uncertainties [14] or the inclusion of parameters. As a rather recent method it lacks the popularity and pervasiveness, as it is the case for the reduction by projection on a reduced basis. Furthermore, the Proper Generalised Decomposition is a monolithic approach and does not allow assembling different methods that respond to the different requirements in a single integrated method depending on the problem at hand.

In the following the nonlinear system and its reduction by projection on a reduced basis is presented in Sect. 2. The Sect. 3 covers the three elements that are to form the integrated method and whose necessity is derived from the inspections of the previous equations and from numerical results. The integrated method is created in Sect. 4. It is assembled from the elements from the previous section and presented in one full cycle. Its application to a finite element test-case and the results are given in Sect. 5. The conclusion is given in Sect. 6.

2 Approaching a reduced order model

The jump-off point for the integrated method is the dynamic equilibrium of a full order, nonlinear, non-conservative, dynamic system which is completely discretised in space [5]. It can be written as

$$\mathbf{M}\ddot{\mathbf{u}} + \mathbf{C}\dot{\mathbf{u}} + \mathbf{g}(\mathbf{u}) = \mathbf{f}_E(t), \tag{1}$$

if a Galilean reference frame can be assumed. This assumption allows concentrating on the nonlinear behaviour of the structure without being hampered by the particularities of a revolving structure.

Overdots represent derivations of the displacements $\mathbf{u}$ with respect to time. The $n \times n$ matrices $\mathbf{M}$ and $\mathbf{C}$ represent the mass and the damping terms, respectively. The damping matrix $\mathbf{C}$ adds an artificial Rayleigh damping on numerical level to the otherwise non-dissipative material. The $n \times 1$ vector $\mathbf{f}_E$ describes the external forces, which are exclusively a function of the time t. Later on, in Sect. 3.3, Eq. (1) will also be made dependent from parameters $\boldsymbol{\mu}$. For now, this dependency is dropped for readability.

All nonlinearities are regrouped in the $n \times 1$ vector $\mathbf{g}(\mathbf{u})$, which is an exclusive function of the displacements $\mathbf{u}$. In addition to the exclusive dependency on the displacements, the nonlinear forces are required to be smooth. This excludes e.g. nonlinearities due to contacts. Beyond the assumption of finite displacements no other nonlinearities are considered.

For this case it is assumed that the vector $\mathbf{g}$ represents the Kirchhoff-St. Venant approach to the description of finite deformations. It includes the Green–Lagrange strain and the second Piola–Kirchhoff stress formulations and a hyperelastic material law ([39] and [5]). In this setting, the nonlinearities become cubic, distributed over the entire structure and moderate. The choice of a linear material law is driven by the requirement for a purely geometrically nonlinear system that is to serve as a test-case.

2.1 Reduction by projection on a reduced basis

The projection on a reduced basis is one of the widely used approaches for reduction in the context structural dynamics. This is understandable, as some reduced bases do have a physical meaning and contribute thus not only to the solution itself, but also to the interpretation of the problem. It is a modular approach with a clear separation of the reduction and the solution of the reduced system. This implies that a suitable integration scheme can probably be found for any given problem and, if formulated correctly, this integration scheme does not distinguish between the ROM and the FOM. A reduced basis can be chosen which provides an optimal performance for the problem at hand and which can be readily adapted in size. The modular character of the reduction by projection approach also allows focusing the necessary adaptations either on the reduced basis or on the algorithm for obtaining the transient solution.

For the reduction, the flat space, onto which Eq. (1) is projected is represented with the reduced basis as the $n \times r$ matrix $\boldsymbol{\Phi}$. The $r \ll n$ is the order of the ROM. The physical displacements $\mathbf{u}$ are expressed in the reduced basis $\boldsymbol{\Phi}$ with

$$\mathbf{u} = \boldsymbol{\Phi}\mathbf{q}, \tag{2}$$

where the $r \times 1$ vector $\mathbf{q}$ contains the generalised coordinates. Equation (1) can be written in its reduced form

$$\tilde{\mathbf{M}}\ddot{\mathbf{q}} + \tilde{\mathbf{C}}\dot{\mathbf{q}} + \tilde{\mathbf{g}}(\mathbf{q}) = \tilde{\mathbf{f}}_E(t). \tag{3}$$

The $r \times r$ matrices $\tilde{\mathbf{M}} = \mathbf{\Phi}^{\mathrm{T}}\mathbf{M}\mathbf{\Phi}$ and $\tilde{\mathbf{C}} = \mathbf{\Phi}^{\mathrm{T}}\mathbf{C}\mathbf{\Phi}$ and the $r \times 1$ vector $\tilde{\mathbf{f}}_E(t) = \mathbf{\Phi}^{\mathrm{T}}\mathbf{f}_E(t)$ are the direct reduced equivalents of the respective full order terms.

The $r \times 1$ vector of the generalised nonlinear internal forces is $\tilde{\mathbf{g}}(\mathbf{q})$. Unfortunately, such a reduction is not easily feasible. The finite element formulation of $\mathbf{g}(\mathbf{u})$ proves in general to be far too complicated for a direct reduction. The inflation formulation $\tilde{\mathbf{g}}(\mathbf{q}) = \mathbf{\Phi}^{\mathrm{T}}\mathbf{g}(\mathbf{\Phi}\mathbf{q})$ is another formulation to be avoided. While it will be used in a benchmark function later on during this study, it actually only adds the computational cost of repeated vector multiplications to the finite element formulation. The vector $\tilde{\mathbf{g}}(\mathbf{q})$ is a conceptual placeholder for a reduced formulation of the nonlinear internal forces. Such a formulation is of central importance for the transient solution of the ROM with a time-marching algorithm. With such an expression for $\tilde{\mathbf{g}}(\mathbf{q})$, the structures of Eqs. (1) and (3) become identical and the same solution techniques can be used for a FOM as well as for a completely reduced system. The physics of the ROM is identical to the one of the FOM.

2.2 Creating the reduced basis

For the creation of the basis $\mathbf{\Phi}$, there is a variety of methods available. Some common approaches are reviewed by [24]. The method that will be used during this work are normal modes at a given displacement. They work well with the weak and well-behaving geometric nonlinearities and they allow following the deformation of the structure.

Originally, the modal decomposition technique is a method for decoupling coupled linear differential equations ([5]). If only a limited number of these eigenvectors are used for a projection, this method allows for a very efficient reduction (this approach is introduced as Linear Normal Modes (LNM) in [24], based on e.g. [10]). The first application of normal modes to non-linear systems is most probably from [30]. If the modes are constantly or periodically updated during the solution and the reduced basis evolves with the solution, the normal modes are denominated tangent modes in literature (e.g. [22]). In this case the given displacement is chosen to be the current displacement of the solution $\mathbf{u}^{(t)}$. Normal modes at a given displacement use the tangent stiffness matrix

$$\mathbf{K} = \mathbf{K}\left(\mathbf{u}^{(t)}\right) = \left.\frac{\partial \mathbf{g}(\mathbf{u})}{\partial \mathbf{u}}\right|_{\mathbf{u}^{(t)}} \tag{4}$$

for the eigenproblem

$$\mathbf{K}\boldsymbol{\phi}_i = \omega_i^2 \mathbf{M}\boldsymbol{\phi}_i. \tag{5}$$

The projection basis $\mathbf{\Phi}$ is defined as the first r eigenvectors of the of Eq. 5, which are regrouped in a matrix

$$\mathbf{\Phi} = \left[\boldsymbol{\phi}_1, \ldots, \boldsymbol{\phi}_r\right], \tag{6}$$

if the corresponding frequencies ω_i are sorted in increasing order $0 < \omega_1 \leq \cdots \leq \omega_r \leq \cdots \leq \omega_n$.

3 Elements of the integrated method

The three aspects of the rapid, accurate and parameterisable transient solution are assured with the three elements of the integrated method. The elements are presented independently from each other in the following. First the autonomy that ensures the rapidity of the reduced solution is presented, then the update and augmentation that ensures the accuracy. Finally, the interpolation, that allows a parameterisation, is introduced.

3.1 Autonomy for rapidity

For the polynomial formulation of the nonlinear forces the conceptual placeholder $\tilde{\mathbf{g}}(\mathbf{q})$ in Eq. (3) is supposed to be a polynomial of degree 3 in terms of the generalised coordinates $\mathbf{q}$. The polynomial formulation reads

$$\tilde{\mathbf{g}}_p(\mathbf{q}) = \sum_{h=1}^{3} \tilde{\mathsf{A}}^{(h)}\mathbf{q}^{\otimes h}. \tag{7}$$

The $\tilde{\mathsf{A}}^{(h)}$ are tensors in $\mathbb{R}^{r \times r^h}$. From now on reduced nonlinear terms with the index p are used for polynomial formulations.

The degree of this polynomial reflects the fact that the nonlinearities in the nonlinear internal forces $\mathbf{g}(\mathbf{u})$ in Eq. (1) are cubic. Therefore, it seems to be commonly accepted that a degree of three of the polynomial is sufficient for geometrically nonlinear structures [12,27,28]. Especially [27] state that the internal forces of "an arbitrary linearly elastic [...] structure undergoing large deformations", can be expressed analytically as a polynomial of third order in the derivations of the basic functions with respect to the spatial coordinates. This applies without restrictions to the finite elements used in the context of this work, where development hinges on a general Total Lagrangian formulation of the problem.

Because of the fact that the nonlinear internal forces $\mathbf{g}(\mathbf{u})$ in Eq. (1) are cubic a polynomial of third order could actually be an exact representation of the nonlinear internal forces for the full order, finite element system. However, by being applied to the reduced order system, this polynomial becomes an approximation. This status as an approximation would basically allow treating any kind of nonlinearity and so the polynomial approximation is not limited to a specific type of nonlinear finite element. However, from the experience of

the authors, a sensible application of the polynomial approximation would be restricted to smooth and moderate nonlinearities.

3.1.1 Expressing the nonlinear terms

For expressing the kth component in the $r \times 1$ column vector of the reduced nonlinear forces $\tilde{\mathbf{g}}(\mathbf{q})$ [28] propose a polynomial expression. The components of $\tilde{\mathbf{g}}_p(\mathbf{q})$ are given as

$$\tilde{g}_k(\mathbf{q}) = \sum_{i=1}^{r} \tilde{\mathsf{A}}^{(1)}_{ki} q_i + \sum_{i=1}^{r}\sum_{j=i}^{r} \tilde{\mathsf{A}}^{(2)}_{kij} q_i q_j + \sum_{i=1}^{r}\sum_{j=i}^{r}\sum_{m=j}^{r} \tilde{\mathsf{A}}^{(3)}_{kijm} q_i q_j q_m, \tag{8}$$

as the polynomial formulation. It is important to note the ranges of the indices which can be exploited to reduce computational and storage requirements.

The Eq. (8) constitutes a formulation in the displacements as a sum of monomials. Reichel [33] show that a monomial formulation tends to be ill-conditioned, especially if it is reduced with a projection, and other higher order polynomials are to be preferred. However, this would only be the case if the tensors are identified at full order and then reduced with an approach as proposed by e.g. [32]. Here, the tensors are identified directly in their reduced form and a monomial formulation appears to be an applicable and proven approach (e.g. [28]).

The components of the tangent stiffness matrix are defined as the derivation of the kth component of the vector of nonlinear forces $\mathbf{g}_p(\mathbf{q})$ with respect to the hth generalised coordinate

$$\tilde{K}_{kh} = \frac{\partial g_k}{\partial q_h}. \tag{9}$$

Its components are obtained by applying the definition in Eq. (9) to Eq. (8). This yields

$$\tilde{K}_{kh} = \tilde{\mathsf{A}}^{(1)}_{kh} + \sum_{i=1}^{r}\sum_{j=i}^{r} \tilde{\mathsf{A}}^{(2)}_{kij}\left(\delta_{ih} q_j + \delta_{jh} q_i\right) + \sum_{i=1}^{r}\sum_{j=i}^{r}\sum_{m=j}^{r} \tilde{\mathsf{A}}^{(3)}_{kijm}\left(\delta_{ih} q_j q_m + \delta_{jh} q_i q_m + \delta_{mh} q_i q_j\right). \tag{10}$$

The Kronecker symbols δ_{ih}, δ_{jh} and δ_{mh} account for the derivations of quadratic and cubic terms with equal indices with respect to a single generalised coordinate. The notation of the tangent stiffness matrix in the setting of the polynomial formulation reads $\tilde{\mathbf{K}}_p$.

3.1.2 Identifying the tensor elements

The tensors $\mathsf{A}^{(h)}$ for Eqs. (8) and (10) are identified with a moment matching approach by combining different full order static solutions. The following indirect approach is adapted from [28] and requires $\frac{1}{6}\left(r^3 + 6r^2 + 5r\right)$ evaluations of the full order nonlinear forces $\mathbf{g}(\mathbf{u})$.

The tensor $\tilde{\mathsf{A}}^{(1)}$ is the reduced tangent stiffness matrix $\mathbf{K} = \frac{\partial \mathbf{g}(\mathbf{u})}{\partial \mathbf{u}}$. The tangent stiffness matrix can be obtained at different displacements which would form the hinging point for the following moment matching. Following the original approach the hinging point is set to $\mathbf{u}_0 = \mathbf{0}$. The tensor $\tilde{\mathsf{A}}^{(1)}$ becomes the reduced tangent stiffness matrix of the system linearised at the equilibrium. This is exploited by setting

$$\tilde{\mathsf{A}}^{(1)} = \mathbf{\Phi}^{\mathrm{T}} \left.\frac{\partial \mathbf{g}(\mathbf{u})}{\partial \mathbf{u}}\right|_{\mathbf{u}=\mathbf{0}} \mathbf{\Phi} = \mathbf{\Phi}^{\mathrm{T}} \mathbf{K}(\mathbf{u}_0)\, \mathbf{\Phi}. \tag{11}$$

The components of $\tilde{\mathsf{A}}^{(2)}$ and $\tilde{\mathsf{A}}^{(3)}$ can be identified one vector at the time. The vectors of the reduced basis are varied and used as displacements for the evaluation of the full order nonlinear forces $\mathbf{g}(\mathbf{u})$. For the components $\left[\tilde{A}^{(2)}_{ii}\right]$ and $\left[\tilde{A}^{(3)}_{iii}\right]$ with equal indices the variation Δq_i is added and subtracted from the ith generalised coordinate. This allows obtaining the two equations

$$\left[\tilde{A}^{(2)}_{ii}\right] = \frac{1}{2\left(\Delta q_i \Delta q_i\right)}\left(\mathbf{\Phi}^{\mathrm{T}}\mathbf{g}\left(\boldsymbol{\phi}_i \Delta q_i\right) + \mathbf{\Phi}^{\mathrm{T}}\mathbf{g}\left(-\boldsymbol{\phi}_i \Delta q_i\right)\right), \tag{12}$$

and

$$\left[\tilde{A}^{(3)}_{iii}\right] = \frac{1}{\Delta q_i \Delta q_i \Delta q_i}\left(\mathbf{\Phi}^{\mathrm{T}}\mathbf{g}\left(\boldsymbol{\phi}_i \Delta q_i\right) - \mathbf{\Phi}^{\mathrm{T}}\mathbf{K}\boldsymbol{\phi}_i \Delta q_i - \left[\tilde{A}^{(2)}_{ii}\right]\Delta q_i \Delta q_i\right), \tag{13}$$

for each $i \in \{1, \ldots, r\}$. The terms with $\mathbf{\Phi}^{\mathrm{T}}\mathbf{K}\boldsymbol{\phi}_i \Delta q_i$ cancel each other out because they are linear operations.

For the identification of the components $\left[\tilde{A}^{(2)}_{ij}\right]$, $\left[\tilde{A}^{(3)}_{iij}\right]$ and $\left[\tilde{A}^{(3)}_{ijj}\right]$ with two different indices, a total of three equations is necessary. For each pair $j > i$ with $i \in \{1, \ldots, r-1\}$ and $j \in \{i+1, \ldots, r\}$ these equations are defined by combining the variations Δq_i and Δq_j to obtain

$$\left[\tilde{A}^{(2)}_{ij}\right] = \frac{1}{2\left(\Delta q_i \Delta q_j\right)}\left(\mathbf{\Phi}^{\mathrm{T}}\mathbf{g}\left(\boldsymbol{\phi}_i \Delta q_i + \boldsymbol{\phi}_j \Delta q_j\right) + \mathbf{\Phi}^{\mathrm{T}}\mathbf{g}\left(-\boldsymbol{\phi}_i \Delta q_i - \boldsymbol{\phi}_j \Delta q_j\right) - 2\left[\tilde{A}^{(2)}_{ii}\right]\Delta q_i \Delta q_i - 2\left[\tilde{A}^{(2)}_{jj}\right]\Delta q_j \Delta q_j\right). \tag{14}$$

The coefficients $\left[\tilde{A}^{(3)}_{iij}\right]$ are obtained as

$$\begin{aligned}\left[\tilde{A}^{(3)}_{iij}\right] = \frac{1}{2\left(\Delta q_i \Delta q_i \Delta q_j\right)} \Big(\Big(\boldsymbol{\Phi}^{\mathrm{T}} \mathbf{g} \left(\boldsymbol{\phi}_i \Delta q_i \right. \\ \left. + \ \boldsymbol{\phi}_p \Delta q_j \right) - \boldsymbol{\Phi}^{\mathrm{T}} \mathbf{K} \left(\boldsymbol{\phi}_i \Delta q_i + \boldsymbol{\phi}_j \Delta q_j \right) \Big) \\ - \Big(\boldsymbol{\Phi}^{\mathrm{T}} \mathbf{g} \left(\boldsymbol{\phi}_i \Delta q_i - \boldsymbol{\phi}_j \Delta q_j \right) \\ - \boldsymbol{\Phi}^{\mathrm{T}} \mathbf{K} \left(\boldsymbol{\phi}_i \Delta q_i - \boldsymbol{\phi}_j \Delta q_j \right) \Big) \\ - 2 \left[\tilde{A}^{(3)}_{jjj}\right] \Delta q_j \Delta q_j \Delta q_j - 2 \left[\tilde{A}^{(2)}_{ij}\right] \Delta q_i \Delta q_j \Big) . \end{aligned} \tag{15}$$

The coefficients $\left[\tilde{A}^{(3)}_{ijj}\right]$ are eventually obtained by

$$\begin{aligned}\left[\tilde{A}^{(3)}_{ijj}\right] = \frac{1}{\Delta q_i \Delta q_j \Delta q_j} \Big(\boldsymbol{\Phi}^{\mathrm{T}} \mathbf{g} \left(\boldsymbol{\phi}_i \Delta q_i \right. \\ \left. + \boldsymbol{\phi}_j \Delta q_j \right) - \boldsymbol{\Phi}^{\mathrm{T}} \mathbf{K} \left(+ \boldsymbol{\phi}_i \Delta q_i + \boldsymbol{\phi}_j \Delta q_j \right) \\ - \left[\tilde{A}^{(2)}_{ii}\right] \Delta q_i \Delta q_i - \left[\tilde{A}^{(2)}_{jj}\right] \Delta q_j \Delta q_j \\ - \left[\tilde{A}^{(2)}_{ij}\right] \Delta q_i \Delta q_j - \left[\tilde{A}^{(3)}_{iii}\right] \Delta q_i \Delta q_i \Delta q_i \\ - \left[\tilde{A}^{(3)}_{jjj}\right] \Delta q_j \Delta q_j \Delta q_j - \left[\tilde{A}^{(3)}_{iij}\right] \Delta q_i \Delta q_i \Delta q_j \Big) . \end{aligned} \tag{16}$$

The coefficients $\left[A^{(3)}_{ijm}\right]$, with all different indices, are obtained from a single equation, formulated with the three variations Δq_i, Δq_j and Δq_m. For each tripple $m < j < i$, with $i \in \{1, \ldots, r-2\}$, $j \in \{i+1, \ldots, r-1\}$, and $m \in \{j+1, \ldots, r\}$, this gives

$$\begin{aligned}\left[\tilde{A}^{(3)}_{ijm}\right] = \frac{1}{\Delta q_i \Delta q_j \Delta q_m} \Big(\boldsymbol{\Phi}^{\mathrm{T}} \mathbf{g} \left(\boldsymbol{\phi}_i \Delta q_i + \boldsymbol{\phi}_j \Delta q_j + \boldsymbol{\phi}_m \Delta q_m \right) \\ - \boldsymbol{\Phi}^{\mathrm{T}} \mathbf{K} \left(\boldsymbol{\phi}_i \Delta q_i + \boldsymbol{\phi}_j \Delta q_j + \boldsymbol{\phi}_m \Delta q_m \right) \\ - \left[\tilde{A}^{(2)}_{ii}\right] \Delta q_i \Delta q_i - \left[\tilde{A}^{(2)}_{jj}\right] \Delta q_j \Delta q_j \\ - \left[\tilde{A}^{(2)}_{mm}\right] \Delta q_m \Delta q_m - \left[\tilde{A}^{(2)}_{ij}\right] \Delta q_i \Delta q_j \\ - \left[\tilde{A}^{(2)}_{im}\right] \Delta q_i \Delta q_m - \left[\tilde{A}^{(2)}_{jm}\right] \Delta q_j \Delta q_m \\ - \left[\tilde{A}^{(3)}_{iii}\right] \Delta q_i \Delta q_i \Delta q_i - \left[\tilde{A}^{(3)}_{jjj}\right] \Delta q_j \Delta q_j \Delta q_j \\ - \left[\tilde{A}^{(3)}_{mmm}\right] \Delta q_m \Delta q_m \Delta q_m - \left[\tilde{A}^{(3)}_{iij}\right] \Delta q_i \Delta q_i \Delta q_j \\ - \left[\tilde{A}^{(3)}_{ijj}\right] \Delta q_i \Delta q_j \Delta q_j - \left[\tilde{A}^{(3)}_{iim}\right] \Delta q_i \Delta q_i \Delta q_m \\ - \left[\tilde{A}^{(3)}_{imm}\right] \Delta q_i \Delta q_m \Delta q_m - \left[\tilde{A}^{(3)}_{jjm}\right] \Delta q_j \Delta q_j \Delta q_m \\ - \left[\tilde{A}^{(3)}_{jmm}\right] \Delta q_j \Delta q_m \Delta q_m \Big) . \end{aligned} \tag{17}$$

This concludes the identification of all tensor elements which are necessary to describe the reduced nonlinear forces vector. To ensure a successful identification of the tensors two parameters need to be specified. The variations $\Delta\mathbf{q}$ have to correspond to the expected order of magnitude of the generalised coordinates. The reference deformations $\hat{\mathbf{q}}$, that provide the hinging point for the procedure, are set to zero. This is done in preparation for the prestressing in Sect. 3.3, which requires a common reference deformation for the expression of the nonlinear forces. Should this not be required the $\hat{\mathbf{q}}$ can be chosen freely. [8] give instructions for its introduction and selection and report considerable improvements.

3.2 Update and augmentation for accuracy

The update of the reduced basis forms a self-contained block that can be inserted in the solution procedure. After the update of the reduced basis the solution procedures continues without becoming aware of the update and augmentation. An original feature of the proposed update method is the augmentation of the updated basis with physical quantities to smoothen appearing jumps in the displacements, velocities and accelerations. A novel criterion is proposed that triggers the update with a variable frequency. The trigger of choice is the rate of change of the norm of the initial generalised residual. Whenever $\left| \frac{d||\tilde{\mathbf{r}}||}{dt} \right| > \epsilon_r$ an update can be initiated.

The frequency of the update and augmentation is traced with a counter value m. This counter m is set to zero at every update and augmentation and it is increased for every time-step. So, at every instant, the last update and augmentation took place m time-steps ago. A non-constant m, which implies an update and augmentation at a flexible frequency, is desirable. Because every update and augmentation goes with an anewed identification of the reduced tensors it is also desirable to have a counter value of $m \gg 1$ before initiating the following update and augmentation. So the update and augmentation should not be triggered too often during the solution.

The update and augmentation of the reduced basis is performed at the beginning of an instant t. This lets all operations of the solution algorithm, from the predictions, over the iterations to the updates, take place in this new reduced basis.

To begin the update and augmentation at the instant t the current full order deformation is provided by $\mathbf{u}^{(t)} = \boldsymbol{\Phi}^{(t-m\Delta t)} \mathbf{q}^{(t)}_{\text{before}}$ with the current reduced basis that was established at $t - m\Delta t$. The preliminary updated basis $\hat{\boldsymbol{\Phi}}^{(t)}$ is created with the current displacements $\mathbf{u}^{(t)}$ and Eqs. (4) to (6). The preliminary updated basis is of order r, irrespective of the order of the preceding reduced basis $\boldsymbol{\Phi}^{(t-m\Delta t)}$.

The preliminary generalised coordinates are established as

$$\mathbf{q}^{(t)}_{\text{after}} = \left(\left(\hat{\boldsymbol{\Phi}}^{(t)} \right)^{\mathrm{T}} \hat{\boldsymbol{\Phi}}^{(t)} \right)^{-1} \left(\hat{\boldsymbol{\Phi}}^{(t)} \right)^{\mathrm{T}} \mathbf{u}^{(t)} . \tag{18}$$

The preliminary generalised velocities $\dot{\mathbf{q}}^{(t)}_{\text{after}}$ and accelerations $\ddot{\mathbf{q}}^{(t)}_{\text{after}}$ are obtained in an analogous manner. The least-squares sense is used for the preliminary generalised coordinates out of convenience, even though an energy criterion might work better at this stage.

At this point the two sets of generalised coordinates $\mathbf{q}^{(t)}_{\text{before}}$, before the update, and $\mathbf{q}_{\text{after}}$, after the update, coexist at the same instant t. They describe and approximate the unique physical displacements $\mathbf{u}^{(t)}$ with two different bases. Thus, the Eq. (18) results in $\mathbf{u}^{(t)} = \mathbf{\Phi}^{(t-m\Delta t)}\mathbf{q}^{(t)}_{\text{before}} \neq \hat{\mathbf{\Phi}}\hat{\mathbf{q}}_{\text{after}}$, which constitutes a jump in the displacements. These jumps only appear at update frequencies with $m > 1$. The jumps can be extracted. For the displacements they are determined as

$$\triangle\, \mathbf{u}^{(t)} = \mathbf{\Phi}^{(t-m\Delta t)}\mathbf{q}^{(t)}_{\text{before}} - \hat{\mathbf{\Phi}}^{(t)}\mathbf{q}^{(t)}_{\text{after}}. \tag{19}$$

The same operation is performed for the velocities and accelerations too. In order to smooth the solution, the preliminary reduced basis augmented with the jumps. This leads to the $n \times (r+3)$ matrix

$$\mathbf{\Phi}^{(t)} = \left[\hat{\mathbf{\Phi}}^{(t)}, \quad \triangle\, \mathbf{u}, \quad \triangle\, \dot{\mathbf{u}}, \quad \triangle\, \ddot{\mathbf{u}}\right]. \tag{20}$$

The generalised coordinates are augmented accordingly. This augmentation ensures the continuity of physical displacements with

$$\mathbf{q}^{(t)} = \begin{bmatrix} \mathbf{q}^{(t)}_{\text{after}} \\ 1 \\ 0 \\ 0 \end{bmatrix}, \tag{21}$$

of the physical velocities with

$$\dot{\mathbf{q}}^{(t)} = \begin{bmatrix} \dot{\mathbf{q}}^{(t)}_{\text{after}} \\ 0 \\ 1 \\ 0 \end{bmatrix}, \tag{22}$$

and of the accelerations with

$$\ddot{\mathbf{q}}^{(t)} = \begin{bmatrix} \ddot{\mathbf{q}}^{(t)}_{\text{after}} \\ 0 \\ 0 \\ 1 \end{bmatrix}, \tag{23}$$

This links these generalised quantities with the jumps of the augmented reduced basis from Eq. (20). These augmented generalised quantities serve as the initial conditions for the iterations towards the next instant $t + \Delta t$.

The two static matrices $\mathbf{M}$ and $\mathbf{C}$ are reduced with the updated and augmented reduced basis $\mathbf{\Phi}^{(t)}$ in order to correspond to the new generalised coordinates.

The ROM now operates on order $r+3$. Here it is important to note that the order of the ROM is set to r at t_0, the beginning of the transient solution. It increases to $r+3$ during the first update due to the augmentation of the reduced basis. After the first update and augmentation, the order of the ROM remains at $r+3$ for all consecutive updates and augmentations.

The new, augmented generalised state, defined in Eqs. (21) and (22), does not necessarily fulfil the dynamic equilibrium. This condition has no direct influence on the physical solution, because the physical displacements at the instant t are obtained with the generalised coordinates prior to the update in the basis, where convergence is achieved. Furthermore, the new, augmented reduced state serves only as basis points for the predictive values in the solution scheme for the next inner iterations of the solution algorithm towards the instant $t+\Delta t$. However, the condition of disequilibrium might impede the ability of the inner convergence loop of the solution algorithm to converge. Major convergence problems may arise in the case when these values for the reduced quantities are used as basis for the predictive values. Should this become the case, it might be advisable to accept jumps in the accelerations while allowing for the dynamic equilibrium at the instant after the update by adapting the updated and augmented generalised coordinates accordingly.

A major component for stabilising the solution with the updated reduced basis is the retainer. The retainer mechanism limits the frequency of the update of the reduced basis. Directly after the update and augmentation, the value of $\left|\frac{d||\tilde{\mathbf{r}}||}{dt}\right|$ would be well beyond the threshold ϵ_r because the residuals $\tilde{\mathbf{r}}^{(t)}$, before the update, and $\tilde{\mathbf{r}}^{(t+\Delta t)}$, after the update, are defined in different reduced bases. This would immediately trigger another update, which is not desirable. The retainer prohibits an anewed update for a given time. This can be expressed by adding the condition $m \geq m_r$ to the threshold condition of the time derivate of the residual $\left|\frac{d||\tilde{\mathbf{r}}||}{dt}\right| > \epsilon_r$. Both conditions have to be met for the next update to be triggered.

3.3 Interpolation for parameterisation

The necessity to solve a ROM at different operating points arises e.g. when systems are studied that have a wide range of operating points as an intrinsic property, like e.g. turbomachines or whole planes. The external parameters are supposed to be regrouped in the vector $\boldsymbol{\mu}$ which completely describes the operating point of the structure. This operating point might influence all terms of Eq. (1) and also its initial conditions. Several reduced bases $\mathbf{\Phi}_j$ are established at different, known operating points $\boldsymbol{\mu}_j$. The number of these known operating points is supposed to be sufficient. An inter-

polation between these reduced bases is used to obtain the reduced basis $\boldsymbol{\Phi}_0$ at the actual operating point $\boldsymbol{\mu}_0$.

The following approach is taken from [2,3]. They propose a specific interpolation approach. Such a specific interpolation approach is necessary, because the different reduced bases cannot be interpolated directly. The reduced bases are interpolated one column vector at a time in a tangent space. Let $\{\boldsymbol{\phi}_j\}$ be a number of available, precomputed column vectors of the reduced bases corresponding to the known working points $\{\boldsymbol{\mu}_j\}$. The vectors are corresponding to each other, e.g. through having the same place in the order of normal modes under the assumption of equal shapes. If system has to be reduced at a new operating point $\boldsymbol{\mu}_0$, with $\boldsymbol{\mu}_0 \notin \{\boldsymbol{\mu}_j\}$ the associated basis vector $\boldsymbol{\phi}_0$ can be found by the following four-step algorithm.

Among the precomputed bases' vectors one $\boldsymbol{\phi}_k$ is chosen as the origin of the transformation. In the vicinity of the selected origin $\boldsymbol{\phi}_k$ a number of vectors $\boldsymbol{\phi}_i$ is selected $\boldsymbol{\phi}_i \in \{\boldsymbol{\phi}_j\}$ with $i \neq k$, which are designated to partake in the following interpolation.

The transformation into the tangent space is prepared by a singular value decomposition (SVD) of

$$\left(\mathbf{I} - \boldsymbol{\phi}_k \boldsymbol{\phi}_k^{\mathrm{T}}\right) \boldsymbol{\phi}_i \left(\boldsymbol{\phi}_k^{\mathrm{T}} \boldsymbol{\phi}_i\right)^{-1} \rightarrow \mathbf{U}_i \boldsymbol{\Sigma}_i \mathbf{V}_i^{\mathrm{T}} \quad \forall i, \tag{24}$$

with $\mathbf{I}$ as the $n \times n$ identity matrix. Due to the algorithm, which prescribes to treat one column of the reduced bases at a time, the $\boldsymbol{\Sigma}_i$ and $\boldsymbol{\Sigma}_0$ are actually scalar values. The SVD is performed nonetheless, in order to comply with the representation of the original method.

The transformation of the vector $\boldsymbol{\phi}_i$ into the tangent space is then given as

$$\hat{\boldsymbol{\phi}}_i = \mathbf{U}_i \arctan\left(\boldsymbol{\Sigma}_i\right) \mathbf{V}_i^{\mathrm{T}} \quad \forall i. \tag{25}$$

The interpolation proper is now performed with the transformed column vectors $\hat{\boldsymbol{\phi}}_i$. As each of them is associated to an operating point $\boldsymbol{\mu}_i$ appropriate interpolation procedures can be applied to reach $\boldsymbol{\mu}_0$. A possible procedure is a multivariate interpolation with radial basis functions as it is available from e.g. [34]. It yields the interpolated column vector $\hat{\boldsymbol{\phi}}_0$ in the tangent space.

The reverse transformation begins with a SVD of the interpolated vector

$$\hat{\boldsymbol{\phi}}_0 \rightarrow \mathbf{U}_0 \boldsymbol{\Sigma}_0 \mathbf{V}_0^{\mathrm{T}}. \tag{26}$$

Here the same remark with respect to the SVD applies that was already made for Eq. (24).

The interpolated vector $\boldsymbol{\phi}_0$ is obtained with the retransformation

$$\boldsymbol{\phi}_0 = \boldsymbol{\phi}_k \mathbf{V}_0 \cos\left(\boldsymbol{\Sigma}_0\right) + \mathbf{U}_0 \sin\left(\boldsymbol{\Sigma}_0\right). \tag{27}$$

The vector $\boldsymbol{\phi}_0$ can be inserted as the appropriate column vector in the reduced basis $\boldsymbol{\Phi}_0$ associated with the operating point $\boldsymbol{\mu}_0$.

These four steps are repeated for all r column vectors and the final interpolated reduced basis $\boldsymbol{\Phi}_0$ is obtained by assembling all r interpolated column vectors $\boldsymbol{\phi}_0$. The resulting matrix $\boldsymbol{\Phi}_0$ is subjected to a Gram-Schmidt procedure (e.g. [36]) to ensure its orthogonality.

A similar procedure is available for interpolating the symmetric, positive definite matrices $\mathbf{M}$ and $\mathbf{C}$ as a function of external parameters. Based on the same principle of interpolation in a tangent space the transformation (Eqs. (24) and (25)) and the retransformation (Eqs. (26) and (27)) are different for these symmetric, positive definite matrices. More detail is given in e.g. [2].

4 The integrated method

The integrated method combines the three elements from Sect. 3 on the common backbone of a time-marching solution algorithm. One complete time-step cycle is described in the following.

The initial generalised coordinates $\mathbf{q}^{(0)}$, the initial generalised velocities $\dot{\mathbf{q}}^{(0)}$ and the actual operating point $\boldsymbol{\mu}_0$ are supposed to be known. This allows to treat the transient solution of Eq. (3), which is discretised in time, as an initial value problem.

In the following the HHT-α-method from [19] is developed as the backbone of the integrated method. The HHT-α-method is chosen over the classic Newmark method because it offers an improved numerical damping in the high-frequency range, which is beneficial for the used finite element test-case. The HHT-α-method contains the classic Newmark method as a special case.

Tests have been conducted with the "nonlinear Newmark algorithm", as proposed by [23], as the backbone of the integrated method. This successful application demonstrates that the integrated method can be established with different members of the Newmark family of solution algorithms as its backbone. A recent survey of solution algorithms is given by [15].

The necessary adaptation of the HHT-α-method includes the introduction of the polynomial formulation via $\tilde{\mathbf{g}}_p(\mathbf{q})$ and $\tilde{\mathbf{K}}_p(\mathbf{q})$ to ensure the autonomy of the reduced nonlinear terms and the introduction of the two metrics m and $\left|\frac{d||\tilde{\mathbf{r}}||}{dt}\right|$, which govern the update process.

4.1 Providing the initial reduced basis

The initial reduced basis $\boldsymbol{\Phi}$ at $t = t_0$ is a $n \times r$ matrix. It is provided at the actual operating point $\boldsymbol{\mu}_0$ with the interpolation from Sect. 3.3.

4.2 Identifying the initial tensors for the polynomial formulation

The initial tensors for the polynomial formulation are obtained with the initial reduced basis $\mathbf{\Phi}$. The process is described in detail in Sect. 3.1.2.

4.3 Executing the solution

At t_0 the discrete state of the system is completed by obtaining the generalised accelerations

$$\ddot{\mathbf{q}}^{(0)} = \tilde{\mathbf{M}}^{-1}\left(\tilde{\mathbf{f}}_E\left(t_0\right) - \tilde{\mathbf{C}}\dot{\mathbf{q}}^{(0)} - \tilde{\mathbf{g}}_p\left(\mathbf{q}^{(0)}\right)\right), \tag{28}$$

with the initial conditions $\mathbf{q}^{(0)}$ and $\dot{\mathbf{q}}^{(0)}$. The following course of action is valid for advancing from any completely defined state at any t to the next instant $t + \Delta t$.

Prior to continuing the solution, the need for an update of the reduced basis is determined. The update and augmentation of the reduced basis is triggered with the derivation of the residual with respect to time. This requires the current reduced residual

$$\tilde{\mathbf{r}}^{(t)} = \tilde{\mathbf{f}}_E\left(t\right) - \tilde{\mathbf{M}}\ddot{\mathbf{q}}^{(t)} - \tilde{\mathbf{C}}\dot{\mathbf{q}}^{(t)} - \tilde{\mathbf{g}}_p\left(\mathbf{q}^{(t)}\right). \tag{29}$$

This residual is used to approximate the derivation of the initial residual as backward finite difference

$$\left|\frac{d\,||\,\tilde{\mathbf{r}}\,||}{dt}\right| \approx \left|\frac{||\,\tilde{\mathbf{r}}^{(t)}\,|| - ||\,\tilde{\mathbf{r}}^{(t-\Delta t)}\,||}{\Delta t}\right|. \tag{30}$$

Actually, this residual in Eq. (29) is carried over from the converged inner iterations of the preceding time-step. If the current instant is t_0 the $||\,\tilde{\mathbf{r}}^{(t_0-\Delta t)}\,||$ is set to 0.

For a theoretically perfect convergence of the algorithm for each time step this residual is expected to be zero and the difference $||\,\tilde{\mathbf{r}}^{(t)}\,|| - ||\,\tilde{\mathbf{r}}^{(t-\Delta t)}\,||$ should disappear. This is not the case for a real, numerical setting. Hence, this approach is meaningful. It is also valid to use to reduced residual because the norm of the residual in Eq. (29) is a fraction of the initial residual at the beginning of the iterations. This is achieved by testing the convergence relative to the initial residual (refer to Eq. (35) and the discussion of the convergence).

Alongside, the counter for the retainer is increased with

$$m \rightarrow m + 1. \tag{31}$$

If the two conditions $\left|\frac{d||\tilde{\mathbf{r}}_{(i=1)}||}{dt}\right| \geq \epsilon_r$ and $m \geq m_r$ are met the transient solution is paused at this point and a new basis is introduced. This is described in the Sect. 4.3.1, directly below. If no update and augmentation is required, the solution continues directly with its iterative loop in Sect. 4.3.2.

4.3.1 Updating and augmenting the basis

The two metrics $\left|\frac{d||\tilde{\mathbf{r}}_{(i=1)}||}{dt}\right|$ and m that govern the update and augmentation of the reduced basis, are integrated into the HHT-α-method, which operates on the reduced model with autonomous expressions for the nonlinear forces and the tangent stiffness matrix. They trigger and retain the update and augmentation. If an update and augmentation is triggered the process is executed as it is described in Sect. 3.2. This leads to an updated and augmented reduced basis in a $n \times (r + 3)$ matrix.

The new tensors $\tilde{\mathsf{A}}^{(1)}$, $\tilde{\mathsf{A}}^{(2)}$ and $\tilde{\mathsf{A}}^{(3)}$ are identified with the updated and augmented basis of order $r+3$. The identification is described in detail in Sect. 4.2.

It is of utmost importance to understand that with this formulation of the integrated method the anewed identification of the tensors is an online computation, which represents the major part of the numerical effort for updating and augmenting the reduced basis. This is discussed further in Sect. 5.3.

After the update and augmentation the counter for the retainer is reset to $m = 0$. This blocks the update for the following m_r time-steps. Once the update and augmentation has been performed, the HHT-α-method continues without becoming aware of the updated and augmented basis.

4.3.2 Continuing the solution

Regardless of whether an update took place or not, the transient solution is continued with establishing the dynamic equilibrium at the next instant $t + \Delta t$. The HHT-α-method achieves this with an intermediate step at $t + \alpha\Delta t$. An inner loop over the index (i) with Newton–Raphson iterations is initialised with the predictive values

$$\ddot{\mathbf{q}}_{(i=1)}^{(t+\Delta t)} = \ddot{\mathbf{q}}^{(t)} \tag{32}$$

$$\dot{\mathbf{q}}_{(i=1)}^{(t+\Delta t)} = \dot{\mathbf{q}}^{(t)} + \Delta t\ \ddot{\mathbf{q}}^{(t)} \tag{33}$$

$$\mathbf{q}_{(i=1)}^{(t+\Delta t)} = \mathbf{q}^{(t)} + \Delta t\ \dot{\mathbf{q}}^{(t)} + \frac{1}{2}\,\Delta t^2\ \ddot{\mathbf{q}}^{(t)}. \tag{34}$$

While the index i is still in its first loop, the initial generalised residual is extracted

$$\begin{aligned}\tilde{\mathbf{r}}_{(i=1)}^{(t+\Delta t)} = {} & \tilde{\mathbf{f}}_E\left(t + \Delta t\right) - \tilde{\mathbf{M}}\ddot{\mathbf{q}}_{(i=1)}^{(t+\Delta t)} - \tilde{\mathbf{C}}\dot{\mathbf{q}}_{(i=1)}^{(t+\Delta t)} \\ & - \tilde{\mathbf{g}}_p\left(\mathbf{q}_{(i=1)}^{(t+\Delta t)}\right).\end{aligned} \tag{35}$$

It serves to determine the threshold of convergence. The threshold of convergence is determined with $\epsilon\ ||\,\tilde{\mathbf{r}}_{(i=1)}^{(t+\Delta t)}\,||$, where $\epsilon \ll 1$. The iterations are repeated until the current residual drops below the threshold of convergence for an $i > 1$. If the convergence criterion is not met, the iteration index is augmented.

This definition of the threshold of convergence justifies why the criterion for initiating the update and augmentation in Eq. (30) can be formulated with the converged residual. In the worst case the norm of the converged residual is equal to the norm of the initial residual multiplied by ϵ.

The weighted values at $t + \alpha\Delta t$ for the generalised displacements and the generalised velocities are established as

$$\mathbf{q}_{(i)}^{(t+\alpha\Delta t)} = (1-\alpha)\,\mathbf{q}^{(t)} + \alpha\mathbf{q}_{(i-1)}^{(t+\Delta t)}, \tag{36}$$

and

$$\dot{\mathbf{q}}_{(i)}^{(t+\alpha\Delta t)} = (1-\alpha)\,\dot{\mathbf{q}}^{(t)} + \alpha\dot{\mathbf{q}}_{(i-1)}^{(t+\Delta t)}. \tag{37}$$

The current residual is calculated as

$$\tilde{\mathbf{r}}_{(i)} = \tilde{\mathbf{f}}_E\,(t+\Delta t) - \tilde{\mathbf{M}}\ddot{\mathbf{q}}_{(i)}^{(t+\Delta t)} - \tilde{\mathbf{C}}\dot{\mathbf{q}}_{(i)}^{(t+\alpha\Delta t)} - \tilde{\mathbf{g}}_p\left(\mathbf{q}_{(i)}^{(t+\alpha\Delta t)}\right). \tag{38}$$

The current tangent stiffness matrix $\tilde{\mathbf{K}}_p^{(i)}$ is calculated by applying Eq. (10). It is then introduced into the Jacobian of the ROM

$$\tilde{\mathbf{S}}_{(i)} = \tilde{\mathbf{K}}_p^{(i)} + \frac{\gamma}{\beta\,\Delta t}\tilde{\mathbf{C}} + \frac{1}{\beta\,\Delta t^2}\tilde{\mathbf{M}}. \tag{39}$$

The terms γ and β are parameters in the Newmark method that allow for different integration schemes.

The increment of the generalised coordinates $\Delta\mathbf{q}$ is calculated with the Jacobian and the residual from Eq. (38)

$$\Delta\mathbf{q}_{(i)}^{(t+\Delta t)} = \tilde{\mathbf{S}}_{(i)}^{-1}\tilde{\mathbf{r}}_{(i)}. \tag{40}$$

The Newton–Raphson iterations, as they are formulated above, require a full factorisation of the tangent stiffness matrix. As the focus in this work is set on the integration of the polynomial formulation of the nonlinear terms and update and augmentation of the reduced bases this factorisation is accepted. This is particularly the case because the ROM are rather small. Switching to e.g. a quasi-Newton method for numerical performance at this point should be a subtle numerical refinement of the integrated method. Hints for such quasi-Newton methods are given by [25].

With this increment available, the next values for the generalised displacements, velocities and accelerations can be obtained as

$$\mathbf{q}_{(i+1)}^{(t+\Delta t)} = \mathbf{q}_{(i)}^{(t+\Delta t)} + \Delta\mathbf{q}_{(i)}^{(t+\Delta t)} \tag{41}$$

$$\dot{\mathbf{q}}_{(i+1)}^{(t+\Delta t)} = \dot{\mathbf{q}}_{(i)}^{(t+\Delta t)} + \frac{\gamma}{\beta\,\Delta t}\Delta\mathbf{q}_{(i)}^{(t+\Delta t)} \tag{42}$$

and

$$\ddot{\mathbf{q}}_{(i+1)}^{(t+\Delta t)} = \ddot{\mathbf{q}}_{(i)}^{(t+\Delta t)} + \frac{1}{\beta\,\Delta t^2}\Delta\mathbf{q}_{(i)}^{(t+\Delta t)}. \tag{43}$$

They are used to calculate the residual $\tilde{\mathbf{r}}_{(i+1)}^{(t+\Delta t)}$ and to check the convergence condition

$$||\,\tilde{\mathbf{r}}_{(i+1)}^{(t+\Delta t)}\,|| \leq \epsilon\;||\,\tilde{\mathbf{r}}_{(i=1)}^{(t+\Delta t)}\,||\,. \tag{44}$$

If the convergence condition is not met the index is augmented $i \rightarrow i+1$ and the next iteration is launched by returning to Eq. (36).

If, on the other hand, the convergence is given and Eq. (44) fulfilled, the time is increased

$$t \rightarrow t + \Delta t. \tag{45}$$

and the HHT-α-method returns to Eq. (32) to launch the next time step towards the next instant in time. This is repeated until the end t_e of the simulated time period is reached. The counter m for blocking the update and augmentation is already set in Eq. (31).

5 Application of the integrated method

The application of the integrated method takes place on a three-dimensional test-case with finite elements that are geometrically nonlinear. The elements of the integrated method, as they are presented in Sect. 3, are at first tested independently from each other. While the polynomial formulation of the nonlinear terms enables a rapid solution, the update and augmentation of the reduced basis ensures its accuracy. Treating both elements one at a time allows making a well informed trade-off between rapidity and accuracy in the integrated method, where both elements work in conjunction.

5.1 Describing the test-case

The aim of the introduction of the finite element test-case, is to prove the application of the integrated method to a complex test-case which includes geometrically nonlinear volume elements [21,38]. The turbine blade, which serves as test-case, as it is shown in Fig. 1. It is modelled after a two-dimensional turbine blade used by [37]. Its dynamics can be described entirely with Eq. (1). The blade's geometry describes a twisted cuboid, with neither taper nor curvature. The twist is 36° in positive direction and linearly distributed in radial direction with an untwisted root. Its dimensions with respect to a global axis of rotation are

- $L_z = 4$ for the length of the blade in radial direction,
- $L_x = 2$ for the width of the blade in axial direction,
- $L_y = 1$ for the thickness of the blade in the perpendicular radial direction.

The blade is modelled with 2, 1 and 4 hexahedron elements in x, y and z direction, respectively. Fully clamped at the root this leads to 24 free nodes with 3 translational degrees

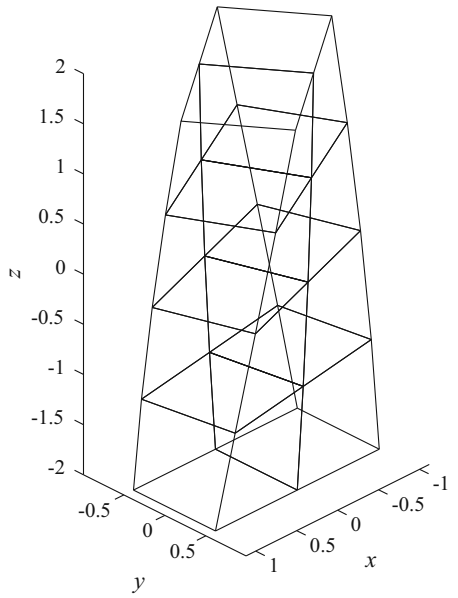

Fig. 1 The geometry of the finite element test-case

of freedom each and to $n = 72$ degrees of freedom for the entire system.

The blade is subjected to a harmonic combined traction and flexion excitation along the $[x, -y, z]$ diagonal of three-dimensional space. The solution takes place between $t_0 = 0$ and $t_e = 5$.

The properties of the blade's material are constant during the solution. Their values are

- $E = 7\ 10^9$ for its Young's modulus,
- $\nu = 0.3$ for the Poisson's ratio, and,
- $\rho = 70$ for the density.

The damping matrix $\mathbf{C}$ in Eq. (1) is obtained by multiplying the tangent stiffness matrix in the equilibrium configuration $\mathbf{K}(\mathbf{u}_0)$ with a factor of $\epsilon = 0.04$. This practice is chosen to avoid a dedicated study of the complex topic of damping without a loss of generality of the integrated method, while, at the same time, stabilising the numerical solution.

The test-case is programmed in MatLab. This allows access down to the level of the numerical integration of individual finite elements. The interpreted programming language is not strictly geared for computational performance and prescribes a limited set of 72 translational degrees of freedom. While this number of degrees of freedom seems limited, it has to be taken into account that a full order reference, finite element solution requires roughly 57 h of computational time. Therefore a reduction is of interest. Furthermore, all performance comparisons take only place within the developed numerical framework. This allows to equate operation counts with computational time and to use only the latter for convenience and accessibility.

Great care has been invested in order to determine the environment for the safe application of the integrated method. For this, the test-case is studied and characterised exhaustively. A convergence study proves that the 72 degrees of freedom are ample for a good trade-off between accuracy and performance. A comparison with the commercial finite element solver NASTRAN is performed and proves the correctness of the developed finite element test-case.

5.2 Performing the interpolation of the reduced basis

The interpolation of the reduced bases, that is developed in Sect. 3.3, is applied to the finite element test-case with nonlinear volume elements. The interpolation serves only to provide the initial reduced basis at the beginning of the transient solution.

In order to impose external parameters, the blade is supposed to be subjected to a prestressing due to a rotation. The rotation is accounted for only in the right-hand side of Eq. (1) by imposing a static prestressing load in the simulation. The prestressing also influences through the elastic nonlinearity and load level the tangent stiffness matrix and hence also the modes. This additional external force depends on the parameters of the rotation speed Ω_a and of the distance to the rotation axis r_a.

The rotation is not taken into account in the left-hand side such as the centrifugal softening or the gyroscopic matrix [4]. This is consistent with the assumption of a Galilean reference frame in Eq. (1), because the gyroscopic coupling and the centrifugal accelerations can be neglected for a constant rotational frequency Ω_a and negligible Coriolis forces. The corresponding skew-symmetric terms do not appear.

The rotation of the blade is supposed to occur around an axis that is parallel to the blade's y axis. The parameters $\boldsymbol{\mu}$ are the prestress radius r_a, the distance of the rotation's axis below the blade's centre of mass, and the rotational frequency Ω_a.

The reduced bases that are used for the interpolation are established with the normal modes at the static displacements $\mathbf{u}_a$ that result from the prestressing at the given operating point $\boldsymbol{\mu}_i = [\Omega_i, r_i]$. The values of $\boldsymbol{\mu}_0$ at the actual operating point to be interpolated are $\Omega_{a,0} = \frac{1}{300}$ per time unit and $r_{a,0} = 5$. The interpolation takes place between precalculated bases. These precalculated bases are obtained with values for the parameters in a rectangular grid with $r_a \in \{2.0, 3.6, 5.2, 6.8, 8.4\}$ and $\Omega_a \in \left\{\frac{1}{120}, \frac{1}{216}, \frac{1}{312}, \frac{1}{408}, \frac{1}{504}\right\}$.

The Fig. 2 shows the first normal modes at $\boldsymbol{\mu}_0$. Its instances are the interpolated mode $\boldsymbol{\phi}_0$ and the reference modes $\boldsymbol{\phi}_{0,\mathrm{ref}}$. The two instances are visually indistinguishable. Together with the numerical results from Table 1 this demonstrates the exceptional quality of the interpolated reduced basis.

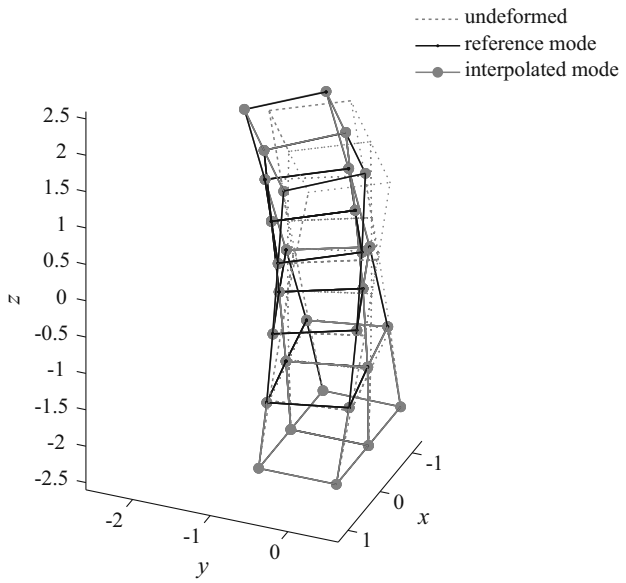

Fig. 2 The interpolation of the first mode of the finite element test-case with volume elements

Table 1 The comparison of the interpolated modes with the reference modes for the finite element test-case with volume elements by means of the MAC

Mode	e_a
1	0.9998
2	0.9999
3	0.9990
4	0.9996
5	0.9999
6	0.9997
7	0.9993
8	0.9995
9	0.9994
10	0.9994
11	0.9994
12	0.9977

Table 1 contains the error metrics of the modal assurance criterion (MAC) $e_a = \frac{|(\boldsymbol{\phi}_{0,\mathrm{ref}})^{\mathrm{T}}\boldsymbol{\phi}_0|^2}{|(\boldsymbol{\phi}_{0,\mathrm{ref}})^{\mathrm{T}}\boldsymbol{\phi}_{0,\mathrm{ref}}||(\boldsymbol{\phi}_0)^{\mathrm{T}}\boldsymbol{\phi}_0|}$ between the reference modes $\boldsymbol{\phi}_{0,\mathrm{ref}}$ and the modes $\boldsymbol{\phi}_0$ that are obtained with the interpolation. The MAC compares the shapes of the modes.

These results show that the interpolation approach is applicable for the test-case. This is a result that had been expected, because the prestressing has only a moderate impact on the shape of the modes of the smooth nonlinearities of the test-case. The interpolation can be used on the present test-case without restriction for preparing and initialising the transient solution. Once the transient solution is underway, the parameterisation of the test case is taken into account by the update of the reduced basis. For simplification the reduced transient solutions in the following section are considered as being initialised with an interpolated reduced basis, without specifically mentioning it.

5.3 Applying the integrated method

With the initialisation of the initial reduced basis settled, the integrated method is applied one remaining element at the time. This allows observing the impact of the introduction of the update and augmentation and of the polynomial formulation separately. Also their possible interactions can be observed.

The different solution schemes are defined with respect to their nonlinear terms - which are either inflated $\tilde{\mathbf{g}}(\mathbf{q}) = \boldsymbol{\Phi}^{\mathrm{T}}\mathbf{g}(\boldsymbol{\Phi}\mathbf{q})$ or polynomial $\tilde{\mathbf{g}}(\mathbf{q}) = \tilde{\mathbf{g}}_p(\mathbf{q})$, as defined in Sect. 3—and with respect to the reduced basis—which is either constant or updated and augmented as described in Sect. 3.2. From these combinations four different solution procedures become possible. The reduced transient solutions are obtained with

- an inflation formulation of the nonlinear terms and a constant reduced basis,
- a polynomial expression of the nonlinear terms and a constant reduced basis,
- an inflation formulation of the nonlinear terms and an updated and augmented reduced basis, and
- a polynomial expression of the nonlinear terms and an updated and augmented reduced basis.

The integrated method is applied as it is presented in Sect. 4. It is built with the polynomial expression of the nonlinear terms and the update and augmentation of the reduced basis. It is the last element in the listing above.

For all four solution schemes, the tensors for the reduced polynomial expression are obtained with the indirect reduced order identification as presented in Sect. 3.1. The reduced basis is constructed from the normal modes with the eigenproblem in Eq. (5).

In the following, the accuracy of the four solutions is treated first. Then the gains in performance are listed. These two properties of the solutions are treated independently in order to allow for well-informed trade-offs between them.

5.3.1 Accuracy

The results for the accuracy of the integrated method are shown exemplarily with $r = 8$ as the order of the ROM.

The selected error metric for gauging the accuracy of the reduced solutions is the relative root mean square error (R2MSE). For a given instant t_j the R2MSE is defined as

$$e_r\left(t_j\right) = \frac{\sqrt{\sum_{i=1}^{n}\left(u_{i,\mathrm{ROM}} - u_{i,\mathrm{FOM}}\right)^2}}{\sqrt{\sum_{i=1}^{n}\left(u_{i,\mathrm{FOM}}\right)^2}} \tag{46}$$

where the $u_{i,\mathrm{ROM}}$ are physical degrees of freedom at the instant t_j that are reconstructed from the reduced solution with Eq. (2) and the $u_{i,\mathrm{FOM}}$ are the degrees of freedom of the full order reference solution at the same instant t_j. The R2MSE is used to judge the difference between the reduced solution and the full order solution at every time step and in an integral sense as the mean over the entire simulated time.

In order to be applicable without restriction, it has to be considered that the metric e_r is only defined in a setting of Euclidian geometry. Translational and rotational degrees of freedom cannot be mixed and the units in which the displacements are measured may influence the norm. The current test-case does not contain any rotational degrees of freedom and the error metrics are applied in order to create a consistency with the practices in the modal community e.g. [9]. Furthermore, the R2MSE offers the advantage of comparing the actual displacements of the reduced and the reference solution. This is an important property, because e.g. the clearance between the tip of the blade and the casing, which is a distance, has to be reproduced correctly by the ROM.

An error metric that is valid with fewer restrictions would e.g. be the relative energy $E\left(t_j\right)$. It is defined as the total energy of a reduced solution $E_t^{(ROM)} = \mathbf{u}^{\mathrm{T}}\mathbf{K}\mathbf{u} + \dot{\mathbf{u}}^{\mathrm{T}}\mathbf{M}\dot{\mathbf{u}}$ at every instant t_j normalised with the peak total energy of the full order reference solution

$$E\left(t_j\right) = \frac{E_t^{(ROM)}\left(t_j\right)}{\max\left(E_t^{(FOM)}\right)}. \tag{47}$$

The minor restriction applied only for the evaluation of E during postprocessing of the transient solutions, again for convenience, is the assumption that the stiffness matrix $\mathbf{K}$, which is used for the potential energy of the system, is constant. This assumption can reasonably be made for the current test-case. The relative energy E is introduced in order to judge the amount of damping that is cut off by the introduction of the reduction. If there is more energy in the ROM than there is in the FOM this might destabilise the solution.

Before descending into the abstraction of the error metrics it is highly worthwhile to inspect the actual physical displacements visually. The physical displacements of the four solutions are shown in Fig. 3 at $t = 1.5$. This instant is chosen as being representative with large amplitude of the deformation, highlighting the differences between the solutions. This figure highlights especially that the solutions come in two groups: solutions with a constant reduced basis and solutions with an update and augmented reduced basis. The integrated method belongs to the second type of solution. The groups of solutions are clearly distinguishable. At the tip of the blade these difference become most obvious. The two solutions that are obtained with a constant reduced basis display a larger deformation than the two solutions that are obtained with an updated and augmented reduced basis. The solutions with an updated and augmented reduced basis are nearly indistinguishable from the reference solution.

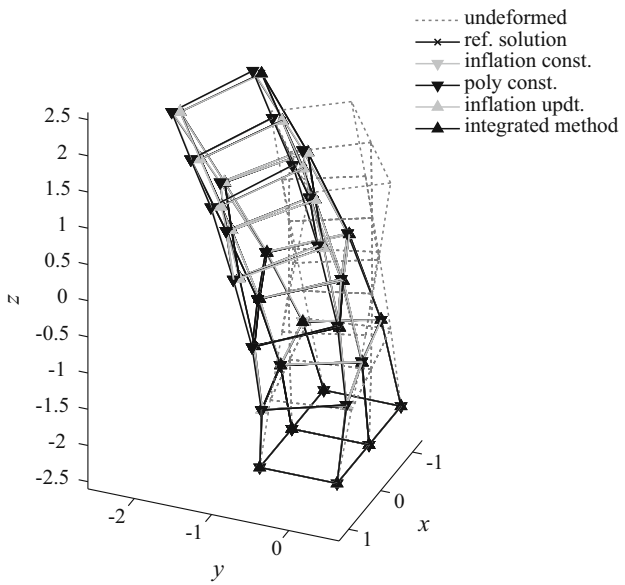

Fig. 3 The physical displacements at $t = 1.5$ of the finite element test-case with volume elements at $r = 8$

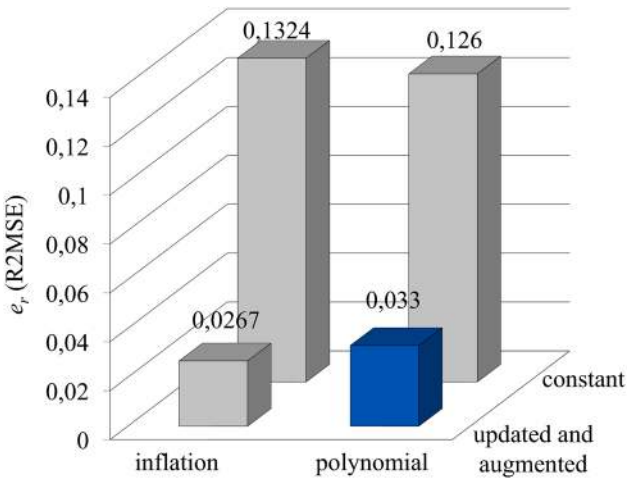

Fig. 4 The R2MSE as a function of the combinations of formulations of the reduced nonlinear forces vector and the reduced basis at $r = 8$

The impression of two groups is confirmed by the inspection of the R2MSE. The Fig. 4 contains the means of the R2MSE for the four solutions. The axes of the horizontal plane of the figure are provided by the combinations of formulations of the reduced nonlinear terms—inflation or polynomial—and the handling of the reduced basis—constant or updated and augmented—, with which the four

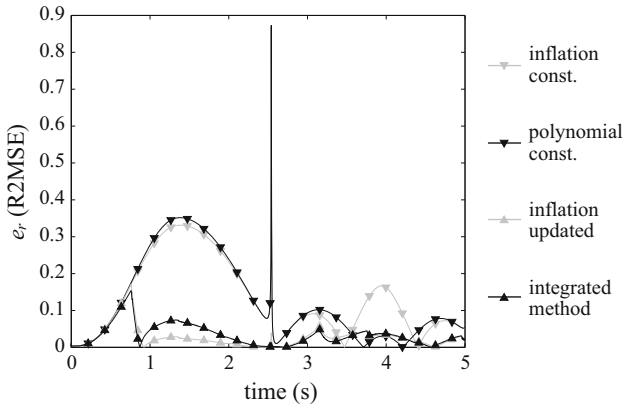

Fig. 5 The evolution of the R2MSE for four solutions of the finite element test-case with volume elements at $r = 8$

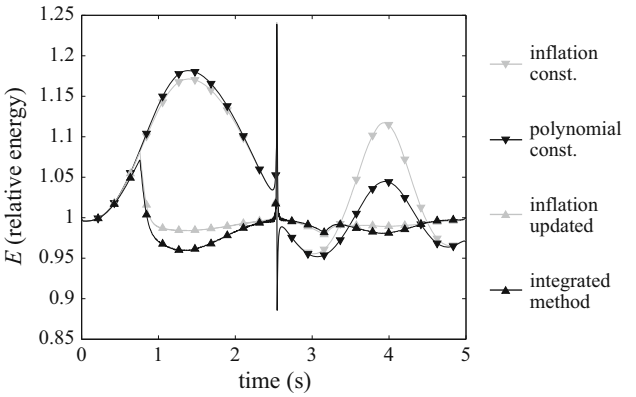

Fig. 6 The evolution of the relative energy for different solutions of the finite element test-case with volume elements at $r = 8$

solutions are obtained. The study of this figure reveals that the update and augmentation of the reduced basis has a significant influence on the quality of the solution, while the influence of the introduction of the polynomial formulation is negligible.

The Fig. 5 traces the evolutions of the R2MSE e_r for the four solutions. The evolutions is generally smooth and follows the amplitude of the displacements of the solution. However, they display prominent spikes when then reference quantity of the reference solution crosses zero. These spikes are purely numerical artefacts and due to the fact that the error metrics are relative ones.

It is remarkable how the R2MSE of the solution obtained with the integrated method evolves. At first it rises with the other R2MSE as the simulation is started. But after the first update and augmentation at $t \approx 0.75$ it drops sharply and is nearly eliminated shortly afterwards. Then, it continues to evolve with a maximum R2MSE of about one fourth of the maximum value of the R2MSE of the solutions with a constant reduced basis. Every new update and augmentation cycle becomes visible as a sharp bend, which realigns the R2MSE with the abscissa, effectively reducing the error and ensuring the result's accuracy. The same behaviour is also displayed by the R2MSE of the solution obtained with the update and augmentation of the reduced basis and the inflation formulation of the nonlinear terms. This indicates that the update and augmentation of the reduced basis is the major reason for an increase of the accuracy for the reduced solution.

The study of the relative energy in Fig. 6 confirms the beneficial influence of the update and augmentation of the reduced basis in the integrated method. For the integrated method the oscillation of the relative energy is much lower than for the solutions with a constant reduced basis. Also, after the first update and augmentation cycle, the total energy in the reconstructed solution of the integrated method is lower than the energy in the full order reference solution. This shows that the update and augmentation introduces an artificial damping that counterbalances the removal of damping due to the cutting off of modes, albeit with a slight overreaction. Looking back at the R2MSE in Fig. 5 proves that this artificial damping does not come at the expense of wrong amplitudes.

The inspection of the physical displacements, the R2MSE and the relative energy shows the considerable improvement that is possible by updating and augmenting the reduced basis. It also shows that for this case this improvement is independent from the formulation of the reduced nonlinear terms. The solution with the inflation formulation and the solution with the polynomial formulation are visually indistinguishable. At the chosen instant in Fig. 3 two update and augmentation cycles took already place. Against the overall simulated period, the positive effect of the update and augmentation is visible from the first update on.

The next step is to focus on the computational performance of the different solutions so that an informed trade-off between speed and accuracy can be made.

5.3.2 Rapidity

The rapidity of the different solutions is measured with the overall solution time. This is possible because all solutions are implemented in the same way and calculated on the same workstation. The considerable uncertainties attached to the measurements of time due to network exchanges and parallel processes on the shared workstations is countered by the strict measurement of CPU time.

The reference solution for measuring the rapidity is the full-order finite element solution. It requires 205430 s of CPU time and provides the touchstone for the reduced solutions. The overall solution times of the solutions whose accuracy is examined in the previous paragraph are shown in the Fig. 7. It uses the same layout as the Fig. 4.

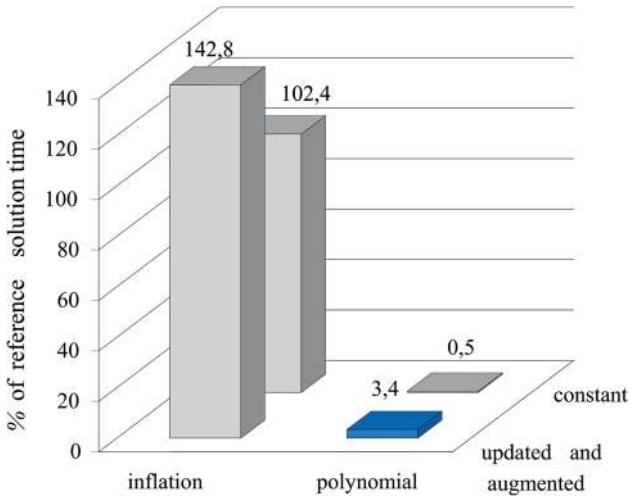

Fig. 7 The relative solution time as a function of the combinations of formulations of the reduced nonlinear forces vector and the reduced basis at $r = 8$

The values in Fig. 7 show very clearly the cost associated with the identification of the polynomial approximation of the nonlinear terms. For the autonomous solution with a constant reduced basis at $r = 8$. The identification of the tensors takes almost one tenth of the time of the full order solution, while the actual solution time becomes negligible. The 0.5 % are distributed as 0.49 % for the identification and 0.01 % for the actual solution among the stages of an autonomous solution with a constant basis. However, when several identifications are required during the updates and augmentations of the integrated method, the times required for each of these identifications in Sect. 4.3.1 is comparable and they add up. The integrated solution requires six identifications, including the initial identification prior to the actual solution. Together, these identifications make the integrated solution take more than 3 % the time of the full order solution.

5.3.3 Trade-off between accuracy and rapidity

In the two preceding sections it is established that the rapidity of the reduced solution depends on the autonomy of the ROM, ensured with the polynomial formulation of the nonlinear terms. The accuracy of the reduced solution is ensured with the update and augmentation of the reduced basis. This update and augmentation entails an anewed identification of the tensors. A process that takes place online and which is rather costly.

The metric of choice for this subject is the number of evaluations of the full order vector $\mathbf{g}(\mathbf{u})$. This vector describes the nonlinear internal forces of the structure for the full order model as a function of the physical displacements. It is provided by the evaluation of the finite element formulation of the full order model.

For the use of the integrated method from Sect. 4, the full order vector of the nonlinear internal forces $\mathbf{g}(\mathbf{u})$ is required by the identification of the reduced tensors $\tilde{\mathbf{A}}^{(h)}$. For the initial identification $\frac{1}{6}\left(r^3+6r^2+5r\right)$ evaluations are required. This number increases to $\frac{1}{6}\left((r+3)^3+6(r+3)^2+5(r+3)\right)$ for each update and augmentation of the reduced basis. The maximum possible number of updates is determined as the maximum number of updates and augmentations during a transient solution $\frac{t_e-t_0}{m_r \Delta t}$, with m_r being the lower threshold of the retainer. This gives the number of required evaluations of the full order nonlinear forces vector $\mathbf{g}(\mathbf{u})$ for the reduced solution as

$$n^{(\mathrm{ROM})}_{\text{evaluations of } \mathbf{g}(\mathbf{u})} \leq \frac{1}{6}\left(r^3+6r^2+5r\right) + \frac{t_e-t_0}{m_r \Delta t}\frac{1}{6}\left((r+3)^3+6(r+3)^2+5(r+3)\right). \tag{48}$$

This is a maximum value because not all updates that are possible during the simulated period $(t_0, t_e]$ are required to take place. It has to be compared to the number of evaluations $n^{(\mathrm{FOM})}_{\text{evaluations of } \mathbf{g}(\mathbf{u})}$ in the full order solution.

The number of evaluations of the nonlinear forces vector $n^{(\mathrm{FOM})}_{\text{evaluations of } \mathbf{g}(\mathbf{u})}$ of the full order solution is given by

$$n^{(\mathrm{FOM})}_{\text{evaluations of } \mathbf{g}(\mathbf{u})} \geq 2\frac{t_e-t_0}{\Delta t}, \tag{49}$$

This value for $n^{(\mathrm{FOM})}_{\text{evaluations of } \mathbf{g}(\mathbf{u})}$ is a lower bound because there can be several iterations per time-step. To comprehend the full numerical effort of the full order solution it has to be understood that it requires additionally an equivalent number of evaluations and factorisations of the full order stiffness matrix. This has to be understood against the background that most of the development of numerical solution schemes is driven by the strive to avoid the creation and inversion of such a stiffness matrix.

The requirements of a trade-off between a rapid and an accurate reduced solution, obtained with the integrated method, is investigated in Fig. 8. In this the figure the solution times from Fig. 7 are plotted against the R2MSE from Fig. 4 for the four different solutions. The solution times are given as percentages of the time required for the full order, reference solution obtained with finite elements. The R2MSE is obtained against the time history result of this reference solution. The solutions included are a solution obtained with a constant reduced basis and the inflation of the nonlinear terms, with a constant reduced basis and the polynomial formulation of the nonlinear terms, with an updated reduced basis and the inflation of the nonlinear terms and a solution obtained with the integrated method. The simulations are performed for orders of the reduced order model of $r = 4$, $r = 8$, $r = 12$ and $r = 16$. The order r of the ROM is colour-coded.

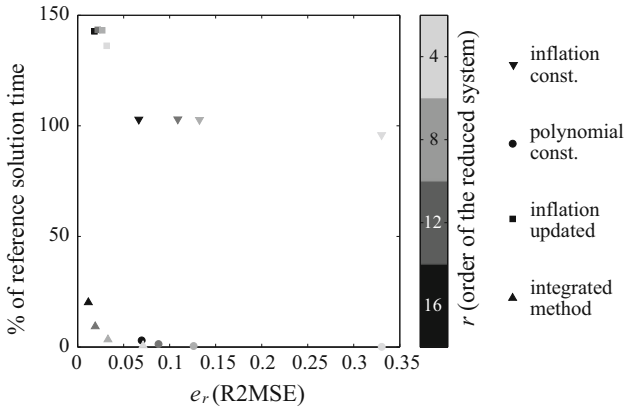

Fig. 8 The R2MSE and solution times of the combinations of formulations of the reduced nonlinear forces vector and the reduced basis

The solutions with a constant reduced basis and the inflation of the nonlinear terms only gain in rapidity from the treatment of the smaller matrices. Because most of the time is spent on the evaluation of the nonlinear terms these solutions take constantly about 100 % of the reference solution's time for all orders r. The same constancy can be observed for the solutions with an updated and augmented reduced basis and the inflation of the nonlinear terms. However, due to the additional effort of the update and augmentation cycle, these solutions require around 140 % of the reference solution's time. Their error level is slightly lower than for the solutions with the constant reduced basis. The solutions with a constant reduced basis and the polynomial formulation of the require constantly below 5 % of the reference solution's time. However, their errors are comparable with the ones of the solutions with a constant reduced basis and the inflation of the nonlinear terms. This confirms that the polynomial formulation does only introduce a small additional error, while accelerating the solution process tremendously.

The solutions of the integrated method stand out, because they display a strong dependency of their solution time on the order r of the ROM. This dependency starts well below 5 % at $r = 4$ and reaches about 20 % at $r = 16$ exponentially. The errors of the solutions obtained with the integrated method are consistent with the other solutions obtained with an updated and augmented reduced basis. At this point it becomes obvious that for the integrated method a large order r of the ROM, which is chosen for accuracy, leads to the imminent danger of negating all possible gains in rapidity, because the numerical effort for the anewed identifications of the tensors scales over-proportionally.

The influence of the identifications becomes highly visible e.g. for $r = 16$. Here, the five updates and augmentations, that take place during the solution, overwhelm the gains due to the use of the polynomial formulation and the time required for the integrated solution raises rapidly and might even approach the time required for the full order solution for $r > 16$. This highlights the computational costs of the identification of the reduced tensors, that are put forward in Fig. 7, and shows how important and difficult it is to make a trade-off between a rapid and an accurate reduced solution. To facilitate this trade-off some rough estimates for the required computational time are given in the Eqs. (48) and (49) above.

Other factors, which are much more difficult to gauge and that depend heavily on the actual implementation of the problem, include the evaluation of the tensor evaluations for the generalised nonlinear forces vector $\tilde{\mathbf{g}}_p(\mathbf{q})$ in Eq. (8) and for the generalised tangent stiffness matrix $\tilde{\mathbf{K}}_p(\mathbf{q})$ in Eq. (10). These evaluations tend to be numerically cheap. They have to be performed the same number of times than the evaluations of the full order terms during the full order solution.

Yet another factor that is difficult to gauge, but beneficial for the ROM, is the requirement to inverse $r \times r$ or $(r+3) \times (r+3)$ matrices instead of $n \times n$ matrices. For this standard problem of linear algebra, many solution approaches exist (see e.g. [36]) and have been implemented with high performance packages in codes as e.g. MatLab or NASTRAN. It has to be determined on a case-by-case basis to which extent the inversion of the smaller matrices unfolds its beneficial effect.

Ultimately it remains out of reach for this study to give an answer that is always valid to the questions for the numerical performance of the integrated method.

6 Conclusion

The central aim of this work is to provide a rapid, accurate and parameterisable transient solution of a geometrically nonlinear structure. This aim is achieved with the creation of the integrated method.

The integrated method is the unification of three different methods on the common backbone of a Newmark-type solution algorithm. Each of the three methods addresses a specific requirement that has been identified and that is commanded by the overall aim of a rapid, accurate and parameterisable transient solution of a geometrically nonlinear structure. Each of the three methods is an example of different common methods that also address the same identified requirement. The method that is actually present in the integrated method is chosen based solely on numerical results. However, any other method that addresses the same identified requirement can replace it in the integrated method. The update and augmentation of the reduced basis is chosen to adapt the solution algorithm in order to make the reduced basis follow the nonlinear evolution of the solution. The polynomial formulation is chosen to form the autonomous expression that replaces the reduced nonlinear terms. The

interpolation in a tangent space is chosen to adapt the initial reduced basis to external parameters.

The study of the performance of the different solutions compares well to the initial assessment of the computational efforts. The influence of the introduction of the polynomial formulation is assessed. All results are confirmed here and especially the potential of the integrated method is again highlighted. The inspection of the results allows distinguishing the impact of the elements of the integrated method. The rapidity is assured with the polynomial formulation and the accuracy with the update and augmentation of the reduced basis. The coactions of these two elements in the integrated method requires a careful trade-off between accuracy and rapidity, because the update and augmentation introduces considerable numerical effort for the anewed identification of the tensors.

The integrated method can be seen as one example of a realisation of an integrated framework. This framework allows for a rapid, accurate and parameterisable transient solutions of a geometrically nonlinear structure.

Acknowledgments The fourth author gratefully acknowledges the support of Alexander von Humboldt Foundation through a Gay Lussac Research Award received in 2013.

References

1. Amabili M (2008) Nonlinear vibrations and stability of shells and plates. Cambridge University Press, New York
2. Amsallem D, Cortial J, Carlberg K, Farhat C (2009) A method for interpolating on manifolds structural dynamics reduced-order models. Int J Numer Methods Eng 80:1241–1258
3. Amsallem D, Farhat C (2008) Interpolation method for the adaptation of reduced-order models to parameter changes and its application to aeroelasticity. AIAA J 46:1803–1813
4. Argyris JH, Mlejnek HP (1991) Dynamics of structures. North Holland, New York
5. Bathe KJ (1996) Finite element procedures. Prentice-Hall, Englewood Cliffs
6. Besselink B, Tabak U, Lutowska A, van de Wouw N, Nijmeijer H, Rixen D, Hochstenbach M, Schilders W (2013) A comparison of model reduction techniques from structural dynamics, numerical mathematics and systems and control. J Sound Vib 332(19):4403–4422. doi:10.1016/j.jsv.2013.03.025
7. Bui-Thanh T, Willcox K, Ghattas O, van Bloemen Waanders B (2007) Goal-oriented, model-constrained optimization for reduction of large-scale systems. J Comput Phys 224(2):880–896. doi:10.1016/j.jcp.2006.10.026
8. Chang YW, Wang X, Capiez-Lernout E, Mignolet MP, Soize C (2011) Reduced order modeling for the nonlinear geometric response of some curved structures. In: International forum of aeroelasticity & structural dynamics (IFASD), Paris
9. Ewins DJ (2000) Modal testing, theory, practice and application, 2nd edn. Research Study Press LTD, Baldock
10. Feeny BF, Liang Y (2003) Interpreting proper orthogonal modes of randomly excited vibration systems. J Sound Vib 265(5):953–966. doi:10.1016/S0022-460X(02)01265-8
11. Galbally D, Fidkowski K, Willcox K, Ghattas O (2010) Nonlinear model reduction for uncertainty quantification in large-scale inverse problems. Int J Numer Methods Eng 81(12):1581–1608. doi:10.1002/nme.2746
12. Grolet A, Thouverez F (2012) On the use of the proper generalised decomposition for solving nonlinear vibration problems. In: ASME 2012 international mechanical engineering congress & exposition, IMECE, Houston
13. Hackbusch W (2012) Tensor spaces and numerical tensor calculus. Springer, Heidelberg
14. Hadigol M, Doostan A, Matthies HG, Niekamp R (2013) Partitioned treatment of uncertainty in coupled domain problems: a separated representation approach. http://arxiv.org/abs/1305.6818v1. Retrieved 8 Nov 2013
15. Har J, Tamma KK (2012) Advances in computational dynamics. Wiley, New York
16. Hay A, Borggaard J, Akhtar I, Pelletier D (2010) Reduced-order models for parameter dependent geometries based on shape sensitivity analysis. J Comput Phys 229(4):1327–1352. doi:10.1016/j.jcp.2009.10.033
17. Hay A, Borggaard JT, Pelletier D (2009) Local improvements to reduced-order models using sensitivity analysis of the proper orthogonal decomposition. J Fluid Mech 629:41–72
18. Hemez FM, Doebling SW (2001) Review and assessment of model updating for non-linear, transient dynamics. Mech Syst Signal Process 15(1):45–74. doi:10.1006/mssp.2000.1351
19. Hilber HM, Hughes TJR, Taylor RL (1977) Improved numerical dissipation for time integration algorithms in structural dynamics. Earthq Eng Struct Dyn 5:283–292
20. Hollkamp JJ, Gordon RW, Spottswood SM (2005) Nonlinear modal models for sonic fatigue response prediction: a comparison of methods. J Sound Vib 284(3–5):1145–1163. doi:10.1016/j.jsv.2004.08.036
21. Holzapfel GA (2000) Nonlinear solid mechanics: a continuum approach for engineering. Wiley, Chichester
22. Idelsohn SR, Cardona A (1985) A load-dependent basis for reduced nonlinear structural dynamics. Comput Struct 20(1–3):203–210. doi:10.1016/0045-7949(85)90069-0
23. Krenk S (2009) Non-linear modeling and analysis of solids and structures. Cambridge University Press, Cambridge
24. Lülf FA, Tran DM, Ohayon R (2013) Reduced bases for nonlinear structural dynamic systems: a comparative study. J Sound Vib 332:3897–3921
25. Matthies HG, Strang G (1979) The solution of nonlinear finite element equations. Int J Numer Methods Eng 14:1613–1626
26. Mignolet MP, Przekop A, Rizzi SA, Spottswood SM (2013) A review of indirect/non-intrusive reduced order modeling of nonlinear geometric structures. J Sound Vib 332(10):2437–2460. doi:10.1016/j.jsv.2012.10.017
27. Mignolet MP, Soize C (2008) Stochastic reduced order models for uncertain geometrically nonlinear dynamical systems. Comput Methods Appl Mech Eng 197:3951–3963. doi:10.1016/j.cma.2008.03.032
28. Muravyov AA, Rizzi SA (2003) Determination of nonlinear stiffness with application to random vibration of geometrically nonlinear structures. Comput Struct 81(15):1513–1523. doi:10.1016/S0045-7949(03)00145-7
29. Newmark NM (1962) A method of computation for structural dynamics. Trans Am Soc Civ Eng 127(1):1406–1432
30. Nickell R (1976) Nonlinear dynamics by mode superposition. Comput Methods Appl Mechanics Eng 7(1):107–129. doi:10.1016/0045-7825(76)90008-6
31. Noor AK (1981) Recent advances in reduction methods for nonlinear problems. Comput Struct 13(1–3):31–44. doi:10.1016/0045-7949(81)90106-1
32. Phillips JR (2003) Projection-based approaches for model reduction of weakly nonlinear, time-varying systems. IEEE Trans Comput Aided Des Integr Circuits Syst 22(2):171–187

33. Reichel L (1985) On polynomial approximation in the complex plane with application to conformal mapping. Math Comput 44:425–433
34. Späth H (1995) Two dimensional spline interpolation algorithms. A.K. Peters, Ltd., Wellesley
35. Spottswood S, Allemang R (2006) Identification of nonlinear parameters for reduced order models. J Sound Vib 295(1–2):226–245. doi:10.1016/j.jsv.2006.01.009
36. Strang G (2006) Linear algebra and its applications, 2nd edn. Thomson, Belmont
37. Tran DM (2009) Component mode synthesis methods using partial interface modes: application to tuned and mistuned structures with cyclic symmetry. Comput Struct 87:1141–1153
38. Wriggers P (2008) Nonlinear finite element methods. Springer, Berlin
39. Zienkiewicz O, Taylor R, Zhu J (2005) The finite element method: its basis and fundamentals. McGraw-Hill, New York